

NPS ARCHIVE
1958
BOAKES, W.

AN INVESTIGATION OF
INFRARED DETECTION BY ELECTRONIC
SCANNING OF A THERMOCOUPLE

WILLIAM H. BOAKES

DUDLEY KNIGHT MARY
NAVAL POSTGRADUATE SCHOOL
MONTEREY CA 93943-5101

AN INVESTIGATION OF INFRARED DETECTION BY
ELECTRONIC SCANNING OF A THERMOCOUPLE

* * * * *

William H. Boakes

AN INVESTIGATION OF INFRARED DETECTION BY
ELECTRONIC SCANNING OF A THERMOCOUPLE

by

William M. Boakes

//

Lieutenant, United States Navy

Submitted in partial fulfillment of
the requirements for the degree of

MASTERS OF SCIENCE
IN
ENGINEERING ELECTRONICS

United States Naval Postgraduate School
Monterey, California

1958

NPS ARCHIVE

1953

BOAKES, W.J.

~~SECRET~~

OK for loan

AN INVESTIGATION OF INFRARED DETECTION BY
ELECTRONIC SCANNING OF A THERMOCOUPLE

by

William H. Boakes

This work is accepted as fulfilling
the thesis requirements for the degree of

MASTER OF SCIENCE

IN

ENGINEERING ELECTRONICS

from the

United States Naval Postgraduate School

ABSTRACT

A new type of IR detector is proposed, employing a short-circuited thermocouple. The design criteria for a short-circuited thermocouple are obtained for specific junction materials (Bi and 95% Bi \neq 5% Sn). The equivalent circuit of the thermocouple is developed and various parameters are computed from which the design curves are made. Feasibility of such an instrument is established conditionally upon the design of a quanta counting indicator.

This thesis was written at the United States Naval Postgraduate School, Monterey, California, during the period January-May 1958. I am indebted to Professor S. H. Kalmbach for his original idea upon which this thesis is based, as well as for his guidance, assistance, and patience as faculty advisor; and to Professor W. P. Cunningham for his valuable assistance.

TABLE OF CONTENTS

Section	Title	Page
1.	Introduction	1
2.	The Detector	3
3.	The Electron Gun	6
4.	The Indicator	9
5.	The Thermocouple	12
5.1	Thermocouple Materials	12
5.2	The Equivalent Circuit	12
5.3	Energy Per Unit Time	17
5.4	Conductance	18
5.5	Thermal Capacity	20
6.	Calculations of Parameters	24
7.	Noise Considerations	29
8.	Summary	33
9.	Bibliography	40
10.	Appendix I	42
11.	Appendix II	47
12.	Appendix III	52

LIST OF ILLUSTRATIONS

Figure		Page
1.	The Detector	4
2.	The Indicator	9
3.	Quanta Measurement	11
4.	The Thermocouple Loop	13
5.	Electrical Equivalent Circuit of the Thermocouple	15
6.	Thermoelectric Equivalent Circuit of the Thermocouple	16
7.	Junction Conductance	19
8.	The Thermal Junction	21
9.	Noise Equivalent Low Pass Filter	30
10.	Time Constant vs Wire Radius	35, 36
11.	Responsivity vs Wire Radius	37
12.	Detectivity vs Wire Radius	38
13.	Figure of Merit vs Wire Radius	39
14.	Magnetic Flux Density vs Loop Radius	45
15.	Electron Beam Displacement vs Wire Radius	46
16.	Critical Length vs Frequency	51
17.	A Comparison of Actual and Approximate Transmission Spectrum of IR Energy	53

TABLES

Number		Page
I	Thermocouple Material Data	25
II	Parameter Variations	34
III	Magnetic Loop Variation	44

TABLE OF SYMBOLS

(Listed alphabetically)

a	area (meter ²) ¹
b	ratio of length to radius
d	diameter of thermocouple loop (meters)
e	electron charge and also base of natural logarithms
g	ratio of receiver to wire radius
h	Planck's constant = 6.625×10^{-34} joule-sec
j	complex operator = $\sqrt{-1}$
k	Boltzmann's constant = 1.38×10^{-23} joule/°K
l	length of wire (meters)
m	mass of electron ($\frac{e}{m} = 1.759 \times 10^{-11}$ coulomb/kg)
r	radius (meters)
s	distance from loop to indicator (meters)
t	time (seconds)
v	velocity (meters/sec)
A	general area (meter ²)
α	thermal admittance (watts/°K)
B	magnetic flux density (webers/meter ²)
C	thermal capacity (joule/°C)
D	range of target (meters)
E	voltage
G	thermal conductance (watt/°K)
I	current (amps)

¹Subscripts are used to denote the material (1-Li; 2-1 - Sn; 3- Cu; 4-Au).

L	critical length (meters)
P	thermoelectric power (volt/ $^{\circ}\text{K}$)
R	electrical resistance (ohms)
R	thermal resistance (watt / $^{\circ}\text{K}$)
T	temperature ($^{\circ}\text{C}$ or $^{\circ}\text{K}$)
V	electric potential (volts)
W	thermal energy per unit time (joules/ sec or watts)
Z	thermal impedance (watt/ $^{\circ}\text{K}$)
θ	angle (degrees)
δ	deflection angle (radians)
ϵ	emissivity ratio (compared with black body)
Θ	angle (degrees)
λ	Constant
μ	microns (10^{-6} meters)
π	Peltier coefficient and 3.14159
ρ	density (kg/ meter ³) and coordinant parameter
σ	Stephan-Boltzmann constant = 5.669×10^{-8} watt/ meter ² - $^{\circ}\text{K}^4$
τ	time constant (sec)
ϕ	angle (degrees)
ω	angular velocity (radians/ sec)

1. Introduction.

Transmission of infrared, IR, energy through the atmosphere is limited to well defined wavelengths (frequencies) with the greatest window between the wavelengths of 8 and 13 microns (10^{-6} meters). The IR spectrum is divided into three regions; the near infrared region, NIR, (0.75 to 1.2 microns), the middle infrared region, MIR, (1.2 to 7 microns), and the far infrared region, FIR, (7 to 1000 microns).

Although the FIR region extends to 1000 microns, the practical limit is now set at approximately 14 microns by the energy and transmission limitations. FIR generally refers only to the 8 to 13 micron window in military applications.

The FIR region contains the peak of energy radiated from a black body between the temperatures of 223° K and 362° K. We are primarily interested in temperatures of 300° K which peak at approximately 10 microns wavelength.

Although much work is presently being done to extend the semiconductor detectors in the FIR region, the best detectors of FIR are still the thermal type (thermocouples, bolometers, etc.).

The targets to be detected are expected to be only a few degrees C above an ambient background which will be taken as 300° K. Of considerable interest are the time of response and the magnitude of the detectable signal, and the effects of noise upon them.

The thermocouple has been used successfully as an IR detector for many years. The normal system of detection utilizes the thermocouple as a source of voltage which is to be amplified and then measured. The idea of making a short-circuited thermocouple to employ the magnetic effects

of the short circuit loop current is apparently original and is the basis for this paper.

The purpose of this investigation is to determine (1) the feasibility of using a short circuited thermocouple loop as a deflection coil of an electron beam to indicate the presence of an IR signal, (2) the conditions and limitations of such an instrument.

This paper is primarily a feasibility study; hence, the results obtained are not expected to be optimum. The optimization is left to future study when and if feasibility has been established.

The MKS system of units is used throughout this paper.

2. The Detector.

The proposed IR detector (Fig. 1) consists of a long electron beam tube with a low velocity electron gun, a thermocouple current loop, and a deflection indicator. These will be discussed separately in subsequent sections.

The IR energy from an extended source is directed onto the thermocouple receiver by double reflection of two front surface reflectors. The first and largest reflector is a spherical mirror of f-number equal to one, which converges the IR rays; the second is a flat mirror of smaller size to direct the converging rays onto the receiver.

The intensity of the source of IR can then be measured (recorded) on the indicator.

Although only a single loop is considered here, it is intended that several loops be used and that the electronic beam sweeps past each loop to give a wide angle of detection.

The field of detection of this instrument is a small solid angle which is a function of the size of the gold foil receiver and the focal length of the spherical mirror. If the source of IR radiation is larger in cross sectional area than the cross sectional area of this solid angle, then a given difference in temperature of the source above the ambient temperature can be detected independent of range. Such a source is sometimes referred to as an extended source.

The energy per unit time that is supplied to the receiver, can be expressed in terms of the f-number, n_f , and receiver area, a_3 , as

$$\Delta W = \frac{\epsilon T^3 \sigma \Delta T a_3}{(n_f)^2} \quad \text{watts} \quad (1)$$

IR source

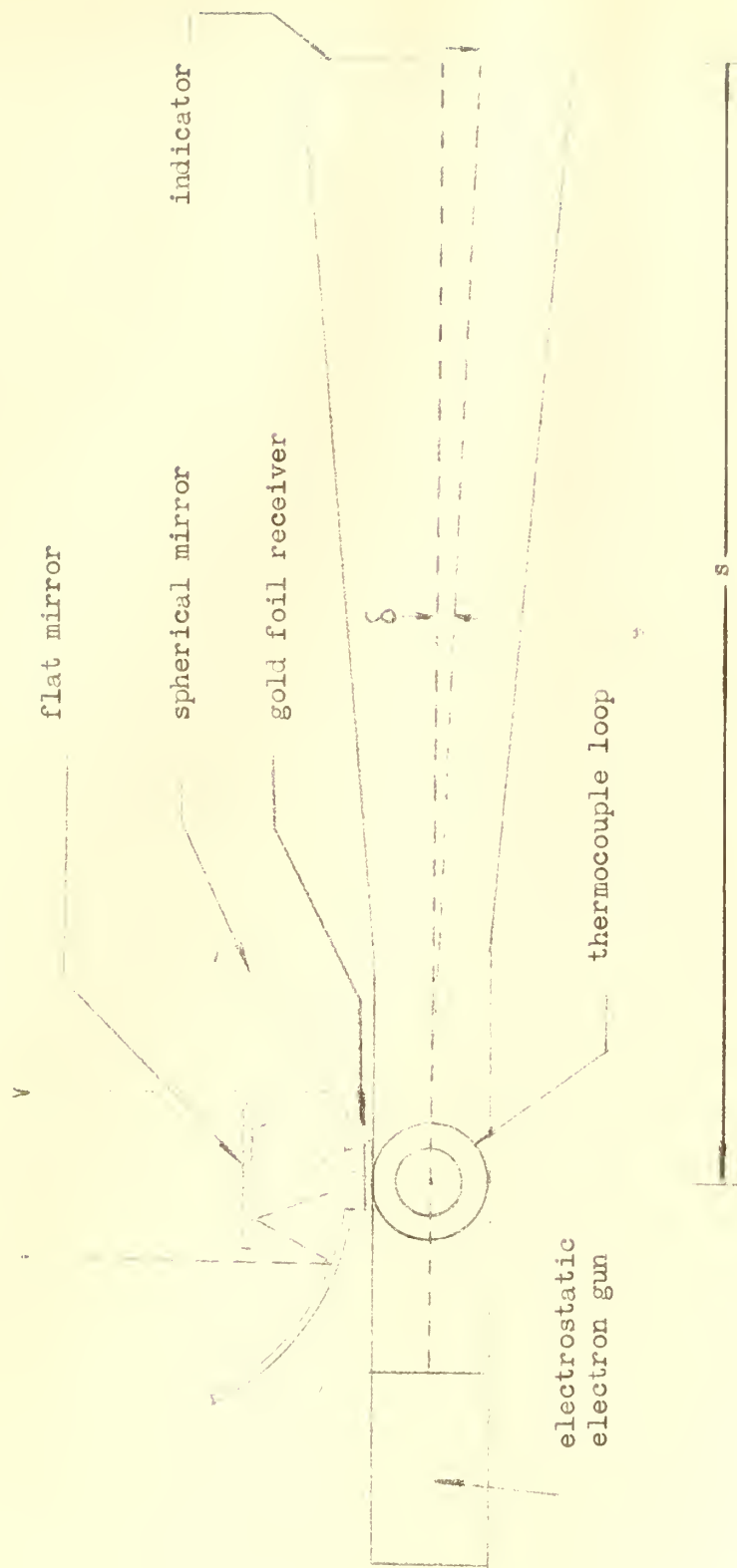


Fig. 1.

Assuming that emissivity, $\epsilon = 1$ (black body) and by construction of the spherical mirror making the f-number equal to one, gives

$$\Delta W = T^3 \sigma \Delta T a_3 \quad \text{watts} \quad (1a)$$

If, however, the cross sectional area of the source is less than the cross sectional area of the solid angle, the detectable signal is range limited and the intensity of the signal decreases as the square of the range. The range of detection is given in this case as

$$D = \frac{r}{2} \sqrt{\frac{\Delta W_s}{\Delta W_D}} \quad \text{meters} \quad (2)$$

where

r = radius of spherical mirror

ΔW_s = power at source

ΔW_D = power on receiver

For signal to noise power equal to one, equation (2) can give the maximum detectable range in this case as

$$D = r \sqrt{\frac{\sigma T^3 \Delta T}{W_N}} \quad (2a)$$

where W_N = noise equivalent power.

3. The Electron Gun.

An electron beam is formed by an electrostatic electron gun. If the accelerating electrostatic field is linear, the beam will emerge with a constant velocity given by

$$v = \sqrt{\frac{2e}{m} V} = 5.93 \times 10^5 \sqrt{V} \quad (3)$$

where v = velocity (meters per sec)

$\frac{e}{m}$ = electron charge to mass ratio (coulombs/kg)

V = electrostatic potential on accelerating anode (volts)

The electron beam of constant velocity is then passed extremely close to the thermocouple loop, causing deflection of the beam. With a current, I , in the loop causing an average magnetic flux density of B webers per square meter across the loop, a deflection angle of the electron beam is

$$\delta = \frac{eBd}{mv}, \text{ radians} \quad (4)$$

where d is the path length (diameter of the loop in meters).

The actual deflection at the indicator is small and can be approximated by

$$y \approx s \delta = \frac{eBsd}{mv} \quad (5)$$

Substituting v from equation (1) gives

$$y = Bsd \sqrt{\frac{e}{2mV}} \quad (6)$$

Taking $s = 1$ meter for convenience

$$y \approx 3 \times 10^5 \frac{Bd}{\sqrt{V}} \quad (7)$$

The average magnetic flux density, B , as a function of loop current, I , has been determined in Appendix I, which gives

$$B = \frac{\mu n I}{\pi d} \quad \text{webers} \quad (8)$$

where n is a function of the distance from the loop to the electron beam. Substituting this into equation (7) we have

$$y = 0.238 \frac{n I}{\sqrt{V}} \quad \text{meters} \quad (9)$$

Although the field of an electrostatic electron gun is not generally uniform, a beam of constant known velocity can be produced which will not differ from the above equations by an appreciable amount.

As the electrons leave the cathode of the electron gun they are deflected toward the axis by a strongly convergent electric field between the grid and cathode. This causes the electron beam to reach a minimum cross-section called "crossover." The radius of this crossover is approximated by Spangenberg⁽¹⁴⁾ assuming a spherical field to give

$$r_o = \frac{2 r_c}{\sqrt{\frac{V_2}{V_e}} \sin 2 \theta} \quad (10)$$

where r_c = radius of cathode

V_2 = potential at crossover

V_e = equivalent voltage of emission velocity

θ = $\frac{1}{2}$ angle of cathode at crossover

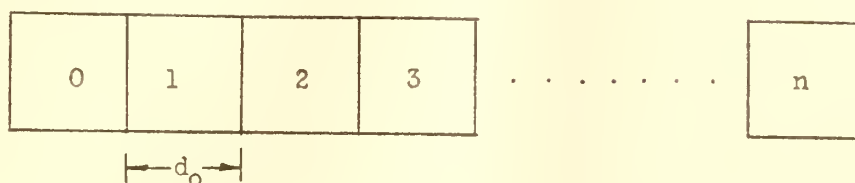
The best spot which can be obtained from the electron beam is formed by focusing this crossover onto the indicating screen. There are various opinions as to what is the actual object of the spot image. The spot is

not the image of the crossover but of a position toward the cathode at which the limiting crossover rays intersect the axis. There is some evidence that this position occurs at the cathode, making the cathode the object. Therefore, the size of the spot equals the size of the cathode. The cathode can be limited in size by using a tungsten wire drawn to the order of 100 microns, thus limiting the spot size.

Equation (9) above does not take into account the fact that the electron beam is a "bundle" rather than a single column of electrons. This bundle of electrons will have a cross-sectional area greater than the spot, since these electrons are convergent as they pass the thermocouple. The actual size of this bundle is difficult to determine. However, by assuming that the electrons are normally distributed across the beam radially so that the standard deviation is equal to the radius of the spot, then computing the deflection of the mean electron of the beam (assuming symmetrical deflection), the approximate deflection can be determined from equation (9).

4. The Indicator.

The size of the spot formed by the electron will determine the minimum detectable deflection which can be achieved. Therefore we will use as an indicator, an array of elements in rectangular form with the side of each element equal to the diameter of the spot.



$$d_0 = \text{cathode diameter} = \text{spot diameter}$$

Fig. 2

Referring to Fig. 2, the electron beam is focused on zero with the background temperature as the input signal. An IR signal producing a temperature difference $\Delta T = 1^\circ \text{C}$ will cause a deflection on the indicator. Since deflection of the electron beam is directly proportional to temperature difference, a direct measure of the temperature difference between a source and its background can be made.

The type of indicator material will depend upon the purpose of the detection. For direct viewing, a phosphorescent screen might be used in the same manner as a cathode ray oscilloscope. Most phosphors will require an accelerating voltage of greater than 1000 volts for visual sensation. This presents no problem, for such a requirement can be achieved quite easily by post deflection acceleration (i.e. deflect the

beam at a low velocity to give large deflection and then accelerate it with high voltages to give the necessary brilliance on the screen).

For this discussion we will consider an ideal indicator which is in effect an electron or quantum counter. We will assume that the smallest detectable signal will be equal to the noise equivalent power (signal to noise ratio of one), as determined by the Johnson noise of the thermocouple. With the electron beam normally distributed in two dimensions (Rayleigh distribution) and the standard deviation equal to the spot radius, the change in quanta can be determined from the deflection of the mean resulting from the noise equivalent power. This ideal detector will have the form of Fig. 2, but as deflection shifts the mean, the difference in number of quanta in each indicator element will give a direct measure of the intensity of the source.

A practical method of determining the magnitude of such a change is illustrated in Fig. 3. A beam of light can be made to approximate the Rayleigh distribution and adjusted onto a double mirror. The double mirror represents two adjacent elements of the detector which must be made to proper scale of the actual detector. Reflected light intensity from each mirror is then measured with photocells and plotted for various deflection angles, (the smallest increment being that resulting from the noise equivalent power). From the normalized curves, a percent of change in quanta can be made directly. For any given electron beam intensity, the indicator requirements are specifically defined.

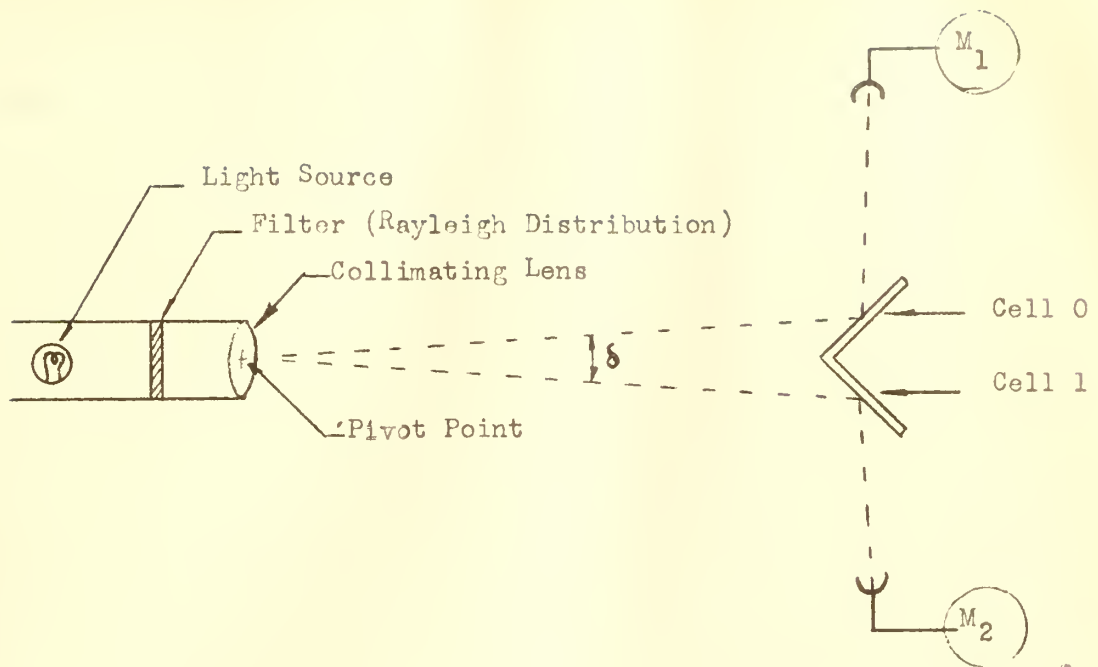


Fig. 3

5. The Thermocouple.

5.1 Thermocouple materials

The heart of the proposed detector is the thermocouple. As shown in Fig. 4, it consists of a thermoelectric junction of bismuth and 95% bismuth plus 5% tin, short circuited by a copper base. These junction materials have been chosen for the following reasons:

(1) These metals produce a junction thermoelectric power of 90 microvolts per degree C, which is quite high.

(2) Each of the elements has a low melting point and, therefore, can be drawn into small wires (20 microns in diameter) by method outlined in Strong⁽¹⁵⁾.

(3) Both metals are soft and easily formed in desired configuration.

The base material can be any good conducting metal, (Ag, Al, Cu); copper has been chosen to give good support and rigidity. The receiver is a thin blackened gold foil with thickness (usually less than one micron) chosen to keep the thermal capacity of the receiver much less than that of the junction metals.

5.2 The equivalent circuit

IR energy from an external source is received on the gold foil via front surface mirrors (Fig. 1). It is assumed that the blackened gold foil acts as a perfect black body and that no reflection occurs. The energy is then transferred to the thermoelectric junction, causing a current to flow in the closed thermocouple loop.

When a current flows between the two dissimilar metals at the junction, a cooling effect is produced at the junction proportional to

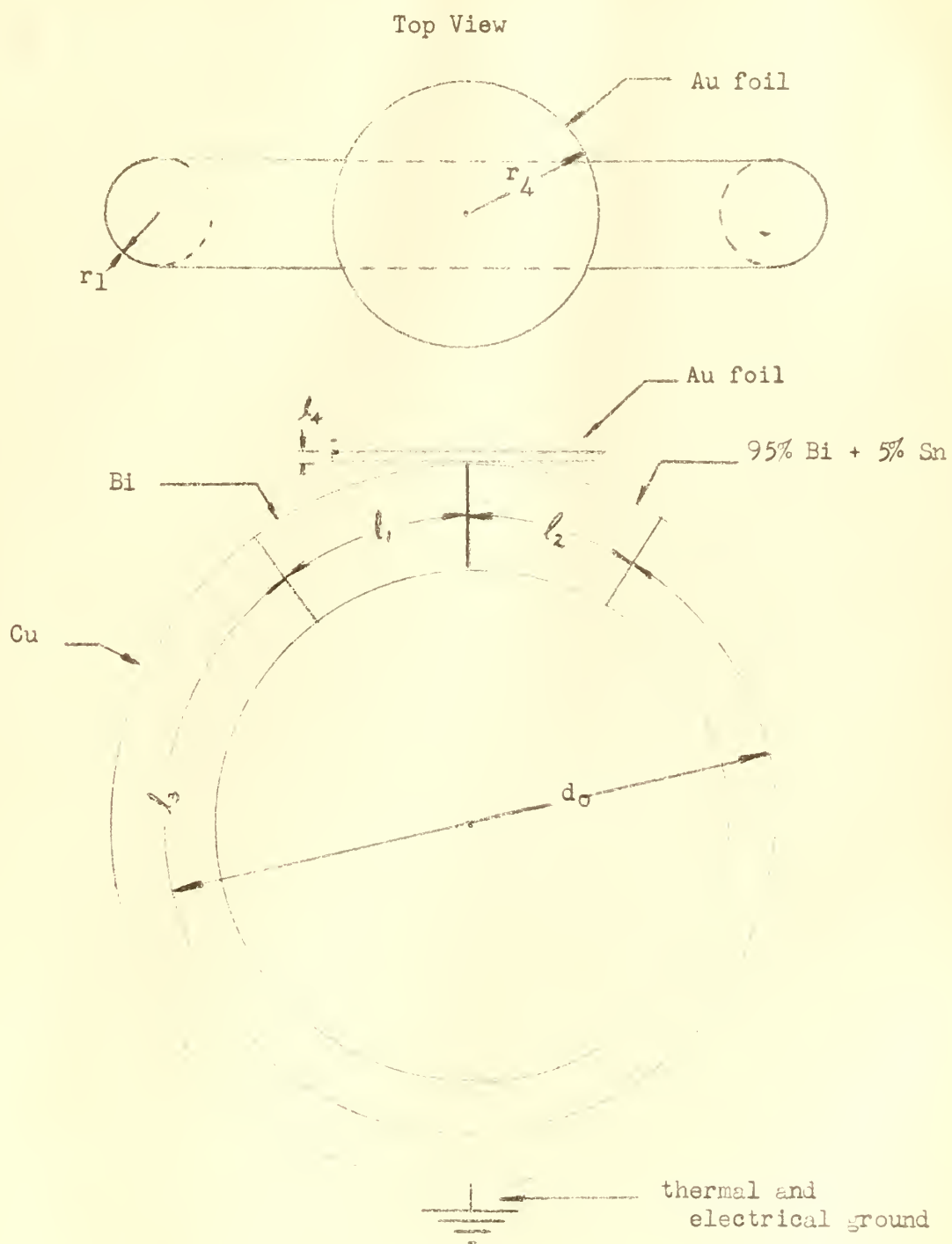


Fig. 4

the current. This effect, first noted by Peltier⁽¹²⁾ is called the Peltier effect. The effect upon the electrical circuit is the same as adding a series resistance, R_d . This is a dynamic resistance since it occurs only when current flows and might be thought of as the internal resistance of the junction.

The change in rate of flow of energy, ΔW , and the change in temperature, ΔT , are related by

$$\Delta W = G \Delta T = \frac{1}{\mathcal{R}} \Delta T \text{ (joules/sec)} \quad (11)$$

where $G = \frac{1}{\mathcal{R}}$ is thermal conductance (watt/°C) and \mathcal{R} is thermal resistance. ΔW caused by Peltier cooling is

$$\Delta W_p = - \pi_j I \quad (12)$$

where π_j , the Peltier coefficient, is equal to the product of the temperature and the thermoelectric power, P , for the junction with the dimension of volts. This gives

$$\Delta W_p = -TPI \text{ (joules/sec)} \quad (13)$$

and a corresponding change in temperature

$$\Delta T_p = -\mathcal{R}TPI \text{ (°C or °K)} \quad (14)$$

This results in a voltage drop

$$E_p = -P \Delta T_p = \mathcal{R}TP^2I \quad (15)$$

from which we find

$$R_d = \mathcal{R}TP^2 \text{ (ohms)} \quad (16)$$

Let E_t = terminal emf (current flowing)

E_o = open circuit voltage

R = electrical circuit resistance

then $E_t = E_o - E_p$ and the loop current $I = \frac{E_t}{R}$

$$\text{then } E_t = IR = E_o - R_d I$$

$$\text{and } I = \frac{E_o}{R + R_d} \quad (17)$$

This gives the equivalent electrical circuit for the short circuited thermocouple as shown in Fig. 5.

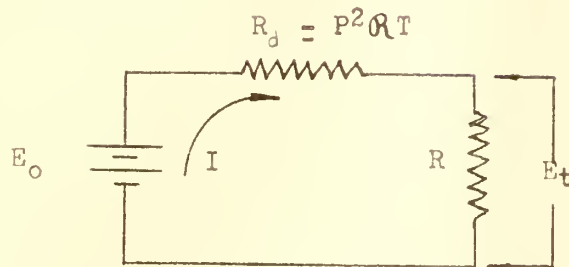


Fig. 5

Relating the electrical circuit to the thermal circuit using

$$E_o = P \Delta T \quad (18)$$

then

$$I = \frac{P}{R + R_d} \Delta T \quad (19)$$

giving loop current as a function of the temperature difference at the junction.

From the energy relationship per unit time, we can determine ΔT .

Energy in = Energy stored + Energy dissipated + Energy radiated.

$$W = \underbrace{C \frac{d \Delta T}{dt}}_{\text{Capacity}} + \underbrace{G_c \Delta T}_{\text{Conduction}} + \underbrace{G_r \Delta T}_{\text{Radiation}} \quad (20)$$

A complete equivalent circuit combining both thermal and electrical properties from equation (20), (17), and (18) is shown in Fig. 6, where an ideal transformer converts thermal energy into electrical energy to satisfy equation (18).

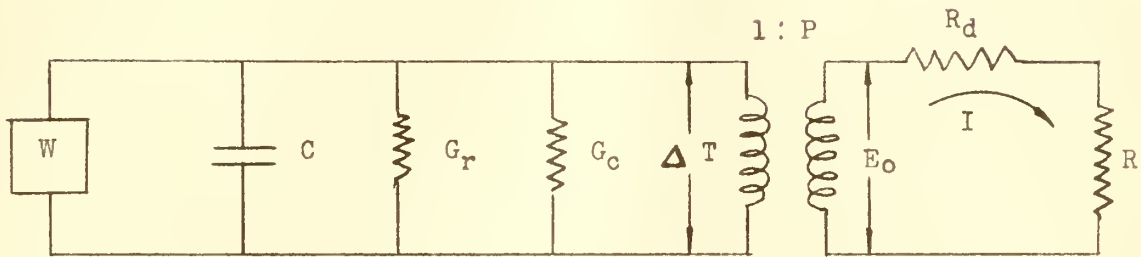


Fig. 6

If W is a step function, then

$$\Delta T = \frac{W}{G} \left[1 - e^{-\frac{t}{\mathcal{R}}} \right] \quad (21)$$

where $\frac{1}{\mathcal{R}} = G = G_c + G_r$, combining like terms of equation (20) and

$$\Delta T \Big|_{t=0} = 0$$

The loop current can now be expressed as a function of time and input energy per unit time by substituting equation (21) in equation (19).

$$I = \frac{P}{R + R_d} = \frac{W}{G} \left[1 - e^{-\frac{t}{RC}} \right] \quad (22)$$

W, G, and C, must now be determined.

5.3 Energy Per Unit Time W (Power).

The curve of transmission bands in the IR spectrum has no specific formula, hence the evaluation of energy in these bands must be approximated by assigning a discrete value (average) over a finite wavelength band, as is shown in Appendix III.

For a black body at 300° K, the energy contained between 8 and 13 microns is approximately 29% of the total energy radiated. Atmospheric absorption reduces the available energy to 20%. The detectable energy below the FIR region is only one-half percent. For practical purposes, all of the detectable energy from a source at T = 300° K is located between wavelengths of 8 and 13 microns.

Assume a black body of area one square meter at a temperature T₁ = 301° K against a background T₀ = 300° K. The total energy radiated from this black body per unit time is

$$W_T = \sigma (T_1^4 - T_0^4) \quad (23)$$

$$\approx 4 \sigma T^3 \Delta T \quad (23a)$$

$$= 6.16 \text{ watts} \quad (23b)$$

Total energy impinging on area A (25 cm. in radius) at a distance, D, from the source is

$$W_A = \frac{AW}{4 \pi D^2} = 0.0963 D^{-2} \text{ watts} \quad (24)$$

but, only 20% of this energy is detectable for any reasonable range of

detection hence

$$W_D = 19.25 D^{-2} \text{ milliwatts} \quad (24a)$$

5.4 Conductance.

The work of Johansen⁽⁵⁾ has given an optimum relation between wire dimensions by maximizing the sensitivity with respect to the ratio of cross section area to length ($\frac{a}{l}$) to yield the following result.

$$\left(\frac{a_1}{l_1} \right)^2 \frac{K_1}{\rho_1} = \left(\frac{a_2}{l_2} \right)^2 \frac{K_2}{\rho_2} \quad (25)$$

$$\frac{l_2}{a_2} = \frac{l_1}{a_1} \sqrt{\frac{K_2 \rho_1}{K_1 \rho_2}} \quad (25a)$$

$$= (0.486) \frac{l_1}{a_1} \text{ for Bi and Bi } \neq \text{ Sn}$$

and $l_2 = 0.486 l_1$, since $a_1 = a_2$

In addition to this, Johansen also found that the losses due to radiation should equal those due to conduction.

$$G_c = G_r$$

$$G_r = 4a_4 \sigma T^3 \text{ (radiation)} \quad (26)$$

The thermal conduction consists of two paths as shown in Fig. 7.

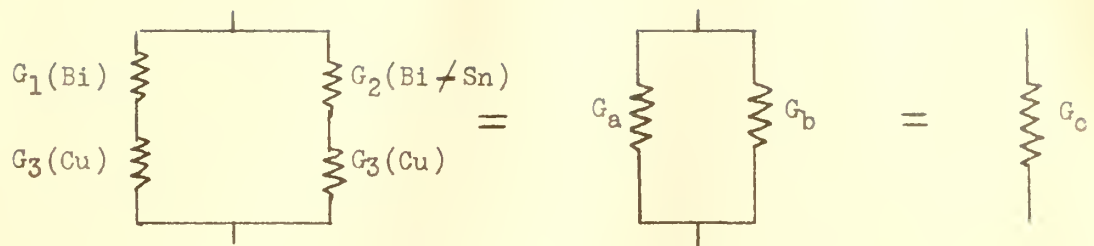


Fig. 7

$$G_o = G_a \parallel G_b \quad (27)$$

$$G_a = \frac{G_1 \parallel G_3}{G_1 \parallel G_3} \quad (27a)$$

$$G_b = \frac{G_2 \parallel G_3}{G_2 \parallel G_3} \quad (27b)$$

where

$$G_1 = \frac{K_1 a_1}{l_1} \quad (28)$$

$$G_2 = \frac{K_2 a_2}{l_2} \quad (28a)$$

$$\text{and } G_3 = \frac{2K_3 a_3}{l_3} \quad (28b)$$

The total conductance follows from equation (20) as

$$G = G_r \parallel G_c \quad (29)$$

Equating equations (26) and (27) and substituting values will yield the relation of radii

$$r_4 = 1.69 \sqrt{\frac{r_1}{b}} \quad (\text{millimeters}) \quad (30)$$

where r_1 is the radius of the wires in microns. There is an order of magnitude of 10^3 between the radius of the gold foil and the radius of the wire if this criterion is used. Since this is quite impractical, this criterion will be ignored.

5.5 Thermal Capacity.

Thermal capacity is equal to the sum of thermal capacities of the gold foil, the blackening, and the junction materials.

$$C_{\text{wire}} = a_1 l_1 C_1 + a_2 l_2 C_2 \quad (31)$$

$$C_{\text{foil}} = a_4 l_4 C_4 \quad (32)$$

When IR energy impinges upon the gold foil receiver, the temperature is raised in an exponential manner in accordance with

$$\Delta T = \Delta T_{\infty} (1 - e^{-\frac{t}{\tau}}) \quad (33)$$

and heat is transferred to the junction. There is an opposition to this transfer of heat which is referred to as thermal impedance, Z , (or its reciprocal thermal admittance, A , such that

$$\Delta T = A \Delta T \quad (34)$$

The flow of heat follows the diffusion equation

$$\frac{\partial \Delta T}{\partial t} = \frac{K}{\rho s} \nabla^2 \Delta T \quad (35)$$

The actual contact area between the gold foil and the junction wires

as shown in Fig. 4, is quite small and the flow of heat from this would be in the form of a spherical wave. The wire being not a right cylinder, but a curved one, adds to the complexity. In order to obtain a reasonable approximation of the flow of heat, the junction can be made as shown in Fig. 8.

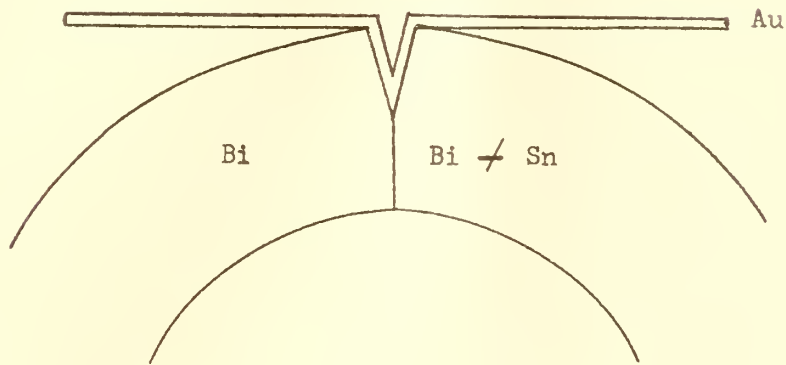


Fig. 8

The following assumptions are made:

- (1) Radiation occurs only at the Au foil; there is no radiation from the wires.
- (2) The wires are right circular cylinders.
- (3) The gold foil transfers energy at the rate ΔW .
- (4) The copper base is at thermal and electrical ground (at a constant temperature).
- (5) The energy is transferred over the cross sectional area of the wires.
- (6) The flow of heat is a plane wave along the axis of the wire.

With these assumptions, equation (35) can now be written in one dimensional form.

$$\frac{\partial \Delta T}{\partial t} = \frac{K}{\rho s} \frac{\partial^2 \Delta T}{\partial x^2}; x = \text{axial direction} \quad (36)$$

with initial conditions for $\Delta T(x, t)$

$$1) \quad \Delta T(l, t) = 0$$

$$2) \quad \Delta T(0, t) = \Delta T(t)$$

which gives the solution, from Appendix II

$$\Delta T(x, t) = \frac{\Delta T(t)}{\sinh \lambda l} \sinh \lambda (l - x) \quad (37)$$

Energy transfer at junction

$$\Delta \dot{Q} = -AK \left(\frac{\partial \Delta T}{\partial x} \right)_{x=0} \quad (38)$$

and

$$\Delta \dot{Q} = Q \Delta T \quad (39)$$

hence from equations (37) and (38)

$$Q = AK \lambda \operatorname{ctnh} \lambda l \quad (39)$$

$$Q \approx \frac{AK}{l} + \frac{AK l}{3} \lambda^2; \text{ for small } \lambda l \quad (40)$$

Two cases are of particular interest. The first, when ΔT is a step function, ΔT is steady when $t > \tau$, and $\frac{\partial \Delta T}{\partial t} = 0$.

The solution to equation (36) is

$$\Delta T(x) = \frac{\Delta T_0}{l} (l - x) \quad (41)$$

From equations (38, 41) we find that

$$Q = \frac{AK}{l} = G \text{ (conductance)} \quad (42)$$

The second case is that of sinusoidal variation in which $W(t) = W_0 e^{j\omega t}$.
Substituting in equation (40) gives

$$a = \frac{AK}{l} + \frac{A l}{3} (j\omega \rho s) \quad (43)$$

$$= G + j\omega C$$

$$G = \frac{AK}{l} \text{ same as steady state equation (42)}$$

$$C = \frac{A l \rho s}{3} \quad (44)$$

This is the practical case which occurs when the radiant IR energy being received is chopped at a frequency $f = \frac{\omega}{2\pi}$ cps. Note that when $\omega = 0$, we have the steady state value $Q = G$, but as ω increases we have an added thermal reactance caused by a thermal capacity of the wires. This new thermal capacity is equal to one-third the thermal capacity of the wires as determined previously from $C = A l \rho s$. This indicates that the thermal capacity when using chopped energy is 4/3 of that when the IR signal is steady.

6. Calculations of Parameters.

The initial design parameters were chosen arbitrarily from practical consideration. Using the method outlined by Strong,⁽¹⁵⁾ the author has successfully drawn wires of both Bi and Bi \nearrow Sn to diameter less than 20 microns. This is considered the smallest practical wire size and is thus chosen as the reference for initial calculations. The wires can be made into a loop of radius three times the radius of the wire which makes the path length $d = 6 r_1$.

$$\text{Bi} \begin{cases} r_1 = 10\mu \\ l_1 = b r_1 = 20\mu; \quad b = 2 \end{cases}$$

$$\text{Bi} \nearrow \text{Sn} \begin{cases} r_2 = r_1 = 10\mu \\ l_2 = .486 \quad l_1 = 9.75\mu \end{cases}$$

$$\text{Cu} \begin{cases} r_3 = r_1 = 10\mu \\ l_3 = \pi d - (l_1 \nearrow l_2) = 160 \end{cases}$$

$$\text{Au} \begin{cases} r_4 = r_1 = 10\mu; \quad g = 1 \\ l_4 = 0.1\mu \text{ (thickness of gold foil)} \end{cases}$$

The electrical resistance of the loop, using values from Table I

$$R = R_1 \nearrow R_2 \nearrow R_3$$

$$R = \frac{\rho_1 l_1}{a_1} \nearrow \frac{\rho_2 l_2}{a_2} \nearrow \frac{\rho_3 l_3}{a_3} \quad (45)$$

$$= 0.17 \text{ ohms}$$

Metal	Resistivity Ohm-meter $\times 10^{-8}$ ρ_l	Thermal Conductivity watts/meter °C K	Thermo- electric Power micro volts/°C P	Electrical Conductivity $\frac{1}{\text{ohm-meter}}$ $\times 10^5$	Specific Heat joule/kg °C S	Density kg/meter ³ $\times 10^3$ ρ	Thermal Capacity joule/meter ³ °C $\times 10^3$ c_s
Bi	120	8.3	-60	8.3	120	9.8	1.18
Bi \neq Sn	275	4.5	7 30	3.6	129	9.33	1.20
Cu	1.72	388		580	391	8.9	3.47
Au	2.44	29.6		410	130	19.3	2.51

This Table was compiled from data given in references [5], [12], [17], [19]

TABLE 1

The thermal conductance consists of radiation and conduction
($G_r \neq G_c$).

$$\begin{aligned} G_r &= 4 \sigma a_4 T^3 \\ &= 1.93 \times 10^{-9} \end{aligned} \quad (46)$$

$$\begin{aligned} G_c &= \text{parallel combination as given by formula (27)} \\ &= 2.52 \times 10^{-4} \end{aligned}$$

Since $G_c \gg G_r$ we can neglect G_r

$$\text{and } G = G_c = 2.52 \times 10^{-4} \quad \text{watts/}^\circ\text{C}$$

Dynamic resistance for a temperature of 300°K is given in equation (15)
as

$$\begin{aligned} R_d &= \frac{P^2 T}{G} \\ &= 0.0097 \text{ ohms} \end{aligned}$$

The current from equation (19) is

$$I_\infty = \frac{P \Delta T}{R + R_d} = 500 \mu\text{a}$$

This current causes a deflection from formula (9) with

$$V = 100 \text{ volts} ; n = \frac{1}{2}$$

$$y = \frac{0.238 I}{4 \sqrt{V}} = 2.98 \times 10^{-6} \quad \text{meters}$$

$$= 2.98 \text{ microns}$$

The thermal capacity is sum of capacities of the junction material, foil,
and blackening from formulas (31, 32)

$$C = 11.15 \times 10^{-9} \quad \text{joules/}^\circ\text{C}$$

which gives a time constant

$$\tau = \frac{C}{G} = 44.3 \mu\text{sec.}$$

This thermocouple has a fast response but low deflection sensitivity.

Detectors have been classified in terms of responsivity, detectivity and figure of merit due largely to the work of R. C. Jones⁽⁶⁾. These terms are now quite common and will be used for this application as defined below.

Responsivity is the ratio of open circuit voltage at the thermocouple to radiant power impinging upon the receiver. If energy is not chopped, the zero frequency responsivity is

$$S_0 = \frac{P \Delta T}{\Delta W} = \frac{P}{G} \quad (48)$$

$$= 0.446 \frac{\text{volts}}{\text{watt}}$$

When radiation is chopped at angular frequency ω the responsivity becomes

$$S(\omega) = \frac{P/G}{[1 + (\omega\tau)^2]^{\frac{1}{2}}} \quad (49)$$

where $\tau = \frac{C}{G}$, time constant of thermocouple.

Detectivity is the ratio of the responsivity to the noise voltage (equation 62a).

$$D_0 = \frac{S_0}{N_0} \quad (50)$$

$$= \frac{0.446}{1.186 \times 10^{-6}} = 3.76 \times 10^5 \text{ (watts}^{-1}\text{)}$$

Where $N_0^2 (= 4 kTR \Delta f)$ the RMS voltage produced by the resistance R. This is called Johnson or thermal noise and is the limiting noise for the

thermocouple.

For chopped radiation

$$D(\omega) = \frac{S(\omega)}{N(\omega)} \quad (51)$$

The figure of merit based on R. C. Jones classification (7) for thermal detectors is

$$\begin{aligned} M_2 &= \frac{D_0}{3.3 \times 10^9} \quad (\text{ratio}) \\ &= \frac{3.76 \times 10^5}{3.3 \times 10^9} = 1.14 \times 10^{-4} \end{aligned} \quad (52)$$

7. Noise Considerations.

The main sources of noise which are encountered are background noise, Johnson or thermal noise, and temperature noise of the junction.

Background noise is quite difficult to define mathematically, but quite easy to determine experimentally. Since we are interested primarily in feasibility study we will consider only a source with definite contrast (i.e. a temperature difference between the source and background at a given background temperature) and leave background noise as a practical consideration for experimentation.

The other two noise sources are contained within the thermocouple loop. Johnson noise results from the Brownian movement of electrons in the circuit resistance which gives a RMS voltage of

$$E^2 = 4kt (\Delta f) R \quad (53)$$

If we think of the electron beam as a single electron of velocity, v , transiting the loop of diameter, d , then the transit time, $t (= \frac{d}{v})$ would be the period during which any thermal fluctuations in the resistor would affect the electron's path. Assuming symmetry of the loop, we can see that for low frequency noise the resulting deflection will be approximately constant during the transit time. As noise frequency increases, we reach a point $f = \frac{1}{2t}$ when the deflection effects are reversed in sign during transit. At this frequency and above, we can see that the noise voltage generated will not affect the deflection.

The loop then acts as a low-pass filter which is assumed to be made up of a series resistance and inductance (Fig. 9).

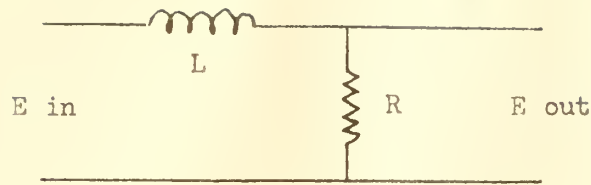


Fig. 9

The bandwidth of this circuit can be determined from the transfer function

$$H(\omega) = \frac{R}{R + j\omega L} \quad (54)$$

$$\left| H(\omega) \right|^2 = \frac{1}{1 + \left(\frac{\omega L}{R}\right)^2} = \frac{1}{1 + \left(\frac{f}{\Delta f}\right)^2} \quad (55)$$

which gives at half power bandwidth

$$\Delta f = \frac{R}{2\pi L} \quad (56)$$

The inductance of a single turn is given in Smythe⁽¹³⁾ as

$$L = b \left[\mu \left(\ln \frac{8b}{a} - 2 \right) + \frac{1}{4} \mu' \right] \quad (57)$$

as used in this loop becomes

$$\begin{aligned} L &= 3r_1 \mu \left[\ln 24 - 2 + \frac{1}{4} \right] \\ &= 3r_1 (4\pi) (3.18 - 1.75) \times 10^{-7} \\ &= r_1 (53.9) \times 10^{-7} \\ &= 53.9 \times 10^{-12} \text{ henrys} \end{aligned} \quad (58)$$

The bandwidth now from equation (56) is

$$\Delta f = \frac{0.179}{2 \pi (53.9) \times 10^{-12}} = 502 \text{ Mcs}$$

The noise voltage is given from equation (53)

$$\overline{E_{NJ}^2} = 1.41 \times 10^{-12}$$

$$\overline{E_{NJ}} = 1.186 \times 10^{-6}$$

and temperature variation

$$\overline{\Delta T_N^2} = \frac{\overline{E_N^2}}{P} \quad (59)$$

$$= \frac{1.41 \times 10^{-12}}{(90)^2 \times 10^{-12}} = 1.74 \times 10^{-4}$$

$$\overline{\Delta T_N} = 1.32 \times 10^{-2} \text{ } ^\circ\text{C}$$

The other noise of interest is the temperature noise occurring at the thermocouple junction as a function of the thermal capacity of the junction materials. This noise causes a temperature fluctuation as given by Fellgett(2).

$$\overline{\Delta T_{NT}^2} = \frac{kT^2}{C} \quad (60)$$

where

$$C = \frac{C_1 C_2}{C_1 + C_2} \quad (61)$$

$$= \frac{(7.41)(3.66)}{10.07} \times 10^{-9}$$

$$= 2.7 \times 10^{-9}$$

and

$$\overline{\Delta T_N^2} = \frac{(1.38)(300)^2 \times 10^{-23}}{2.7 \times 10^{-9}}$$

$$= 4.6 \times 10^{-10}$$

$$\overline{\Delta T_N} = 2.14 \times 10^{-5}$$

This shows that the temperature noise is much smaller than the Johnson noise and can be neglected. The total noise voltage

$$N_o^2 = \sum \overline{E_N^2} \quad (62)$$

gives

$$N_o = \overline{E_{NJ}} = 1.136 \times 10^{-6} \text{ volts} \quad (62a)$$

8. Summary.

Because of the number of variables involved in the investigation, the results are illustrated best by a series of curves. The author has chosen to make the radius of the wire the independent variable for determining various parameters. The relationships of the variables are shown in Table II and are illustrated in Fig. 10 - 13. From the figures, all important characteristics of the thermocouple can be determined directly to meet the desired specifications.

A compromise must always be made between sensitivity and time constant. In order to have a fast response time, one must accept a low order of sensitivity; also conversely.

The feasibility of the detector depends upon the indicator capabilities. If the indicator itself can be made to indicate the quantum change in the deflected electron beam, then the detector is feasible. It will detect a contrast of 1° K at an ambient temperature of 300° K at a distance of greater than 500 meters, if the area of the source is less than the cross sectional area of the solid angle; if the area of the source is greater than the cross sectional area of the solid angle, the detection is independent of range.

The detector can be used with either steady signals or interrupted (chopped) signals of a frequency which can be approximately determined from Fig. 16 of Appendix II. The optimum chopping frequency can best be determined by plotting the frequency response experimentally.

TABLE II

Function		Proportional To	Equations Derived from
Area	a_1	r_1	Definition
length	l_1	br_1	Definition
resistance	R	b/r_1	(45)
conductance	G	r_1/b	(27)
capacity	C	$r_1^{3/b}$	(31,32)
time constant	τ	$r_1^2 b^2$	(47)
responsivity	S_0	b/r_1	(48)
detectivity	D_0	$\sqrt{r_1}$	(50)
figure of merit	M_2	$\sqrt{r_1}$	(52)
deflection	y	n	(8,21)
noise	N_0	$\frac{b}{(r_1)^{3/2}}$	(53,56,57)

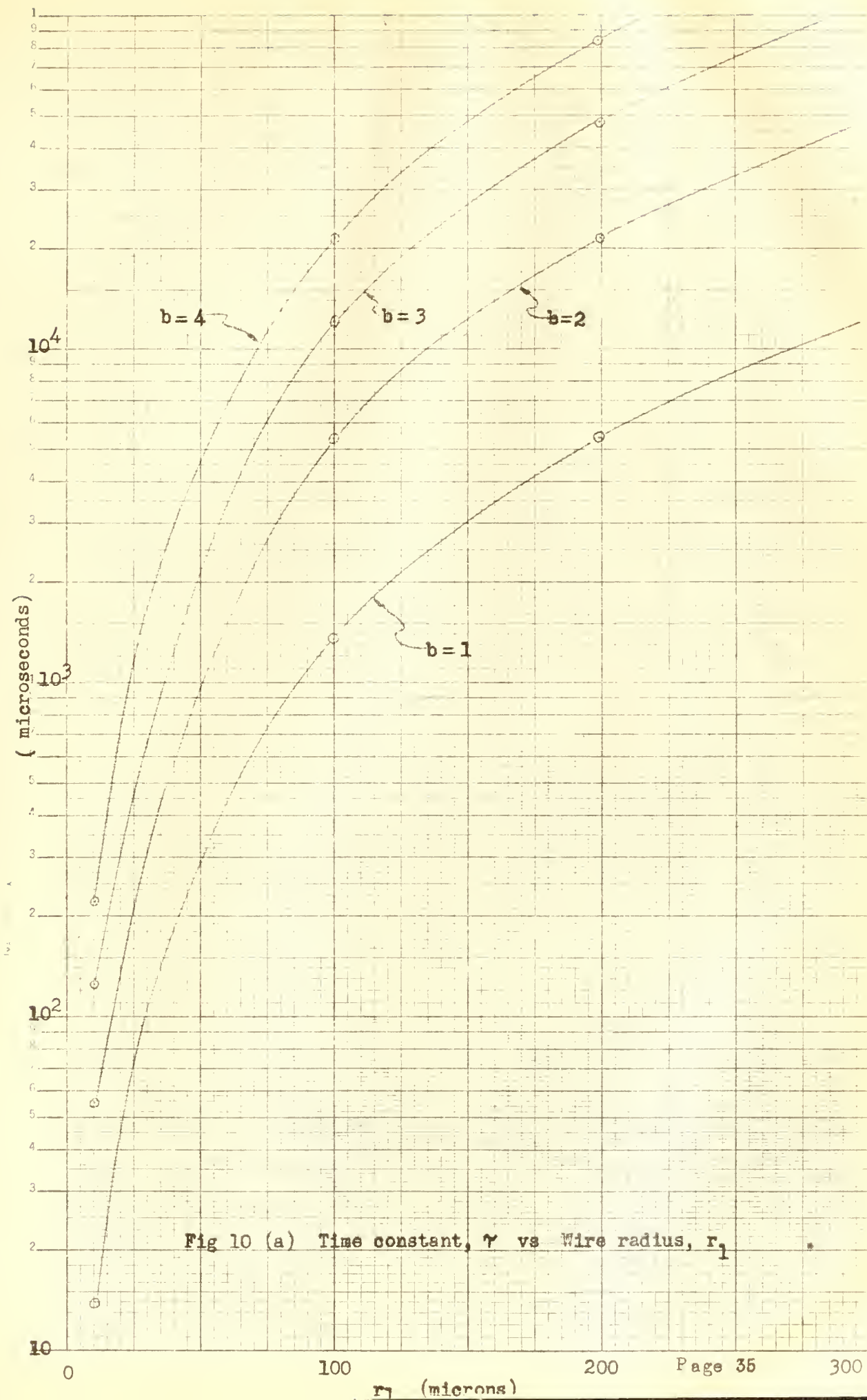


Fig 10 (a) Time constant, τ vs Wire radius, r_1

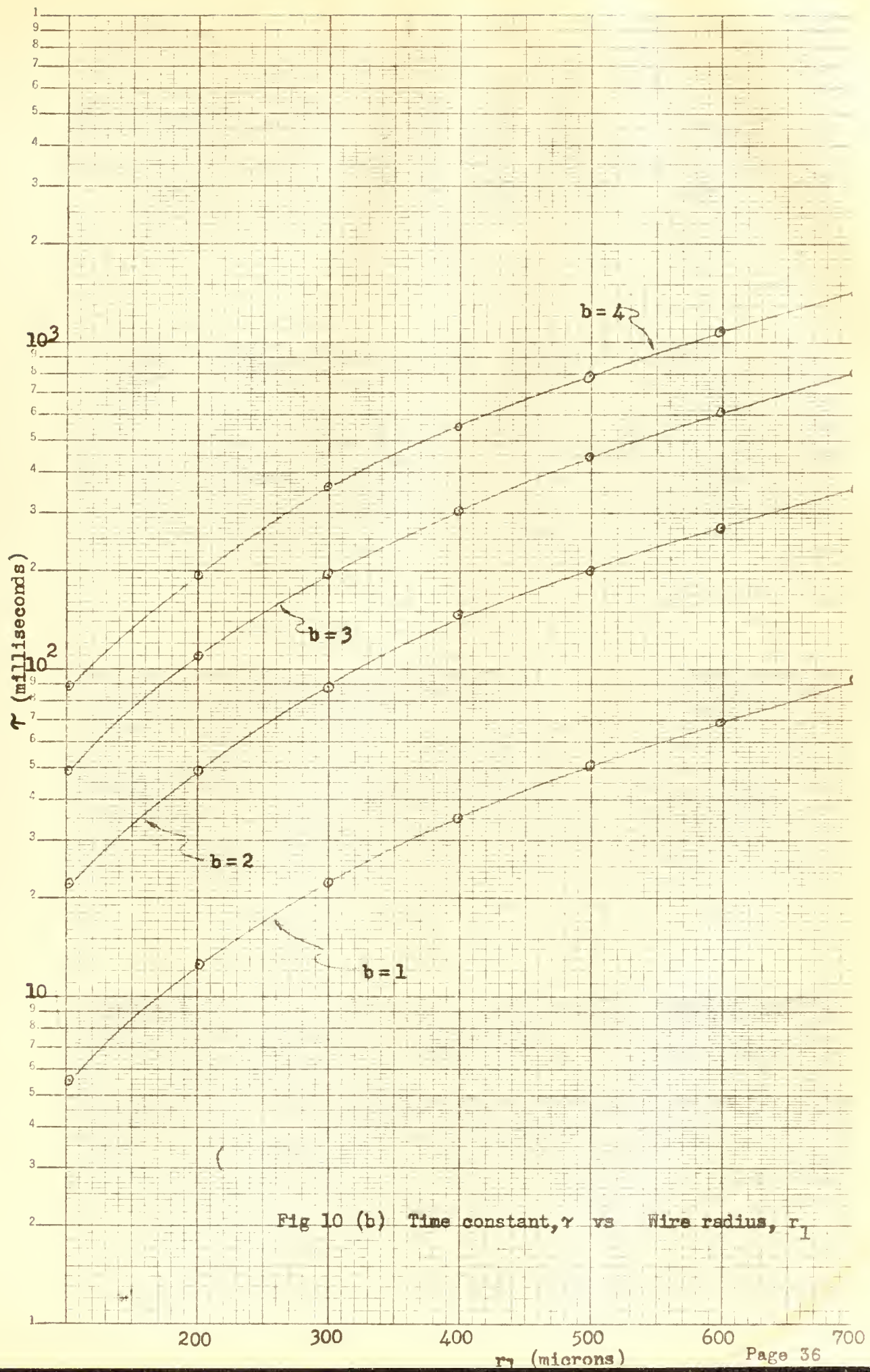
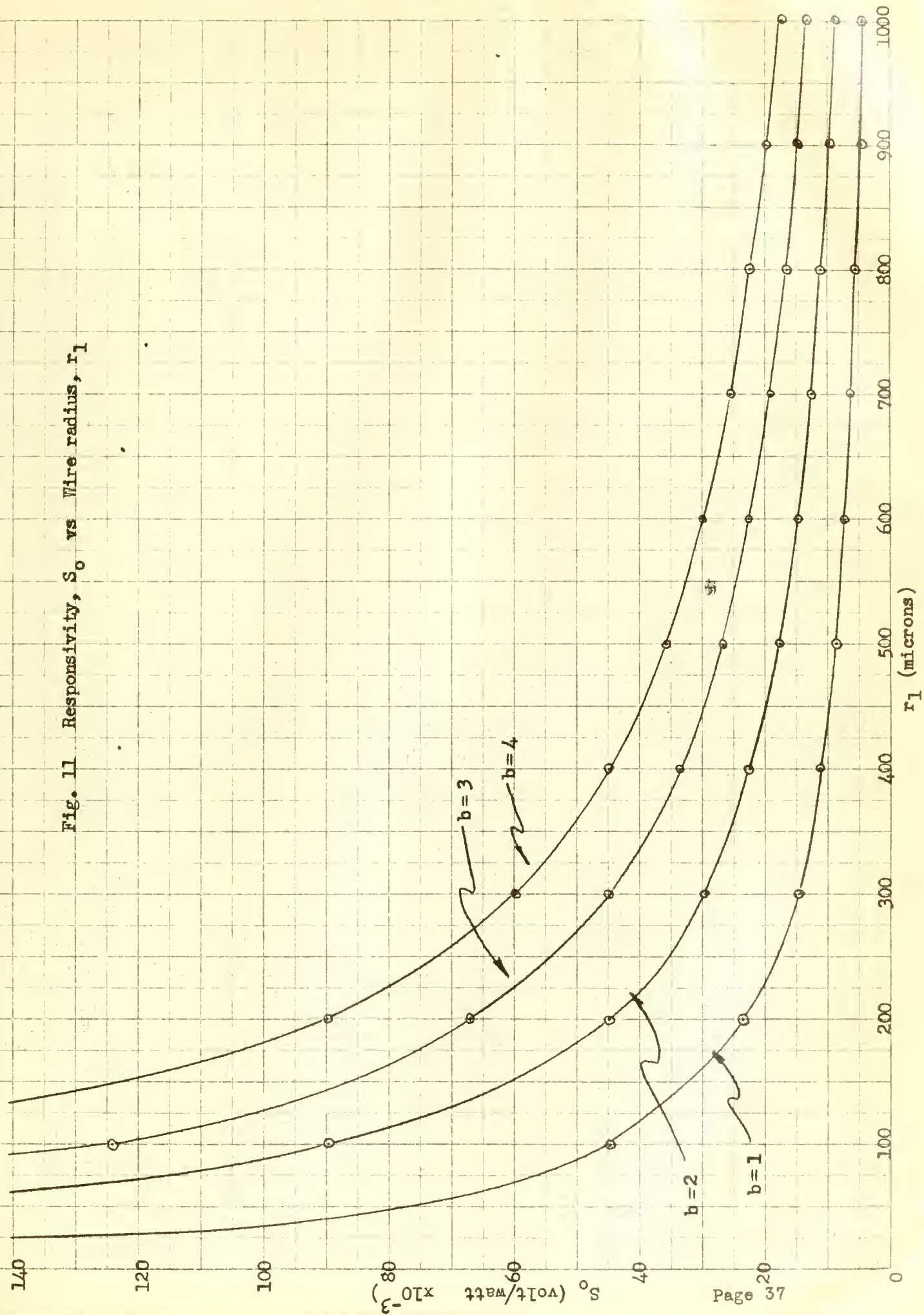


Fig 10 (b) Time constant, τ vs Wire radius, r_1

Fig. 11 Responsivity, S_o vs Wire radius, r_l



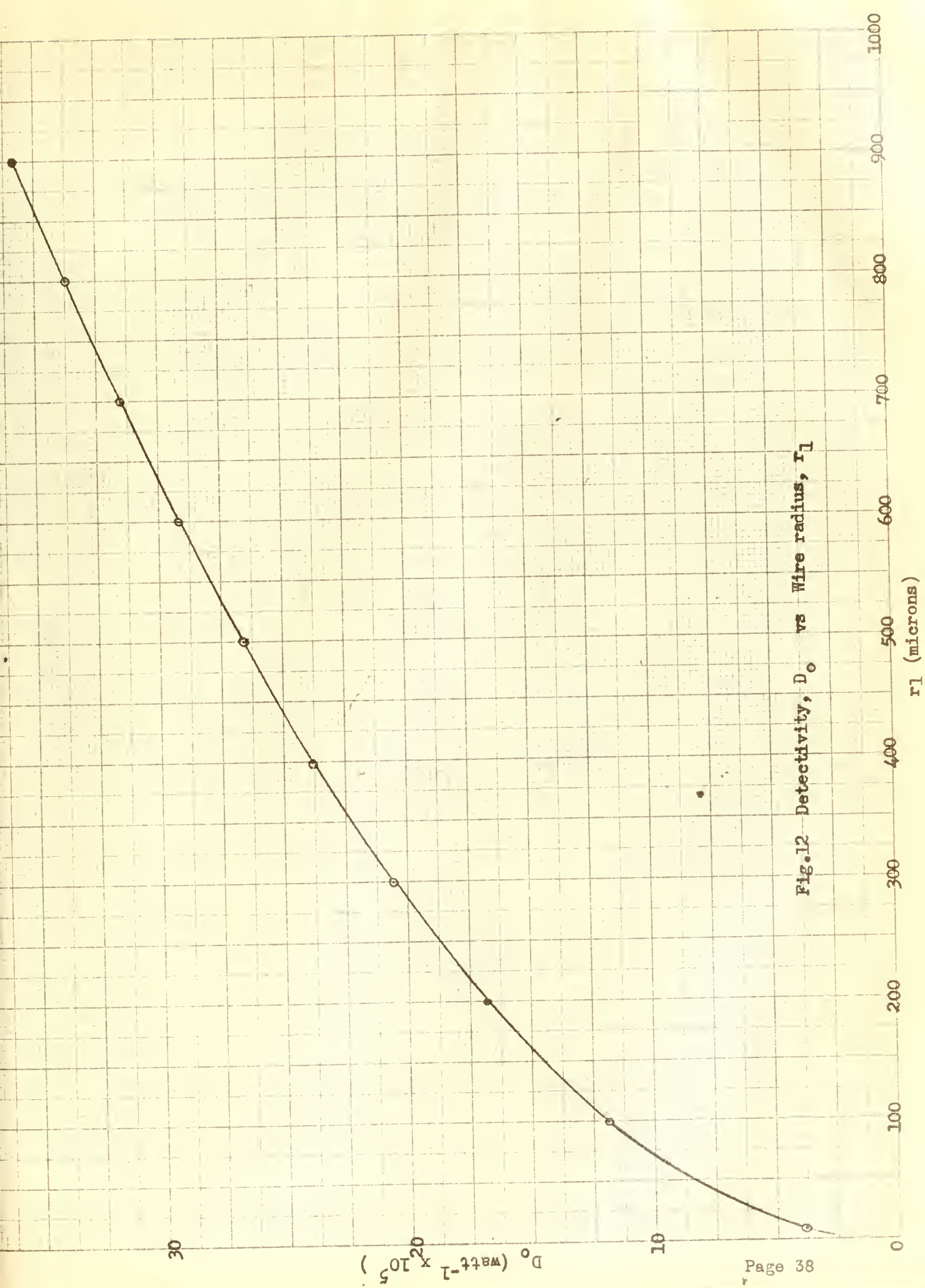


Fig.12 Detectivity, D_o vs Wire radius, r_l

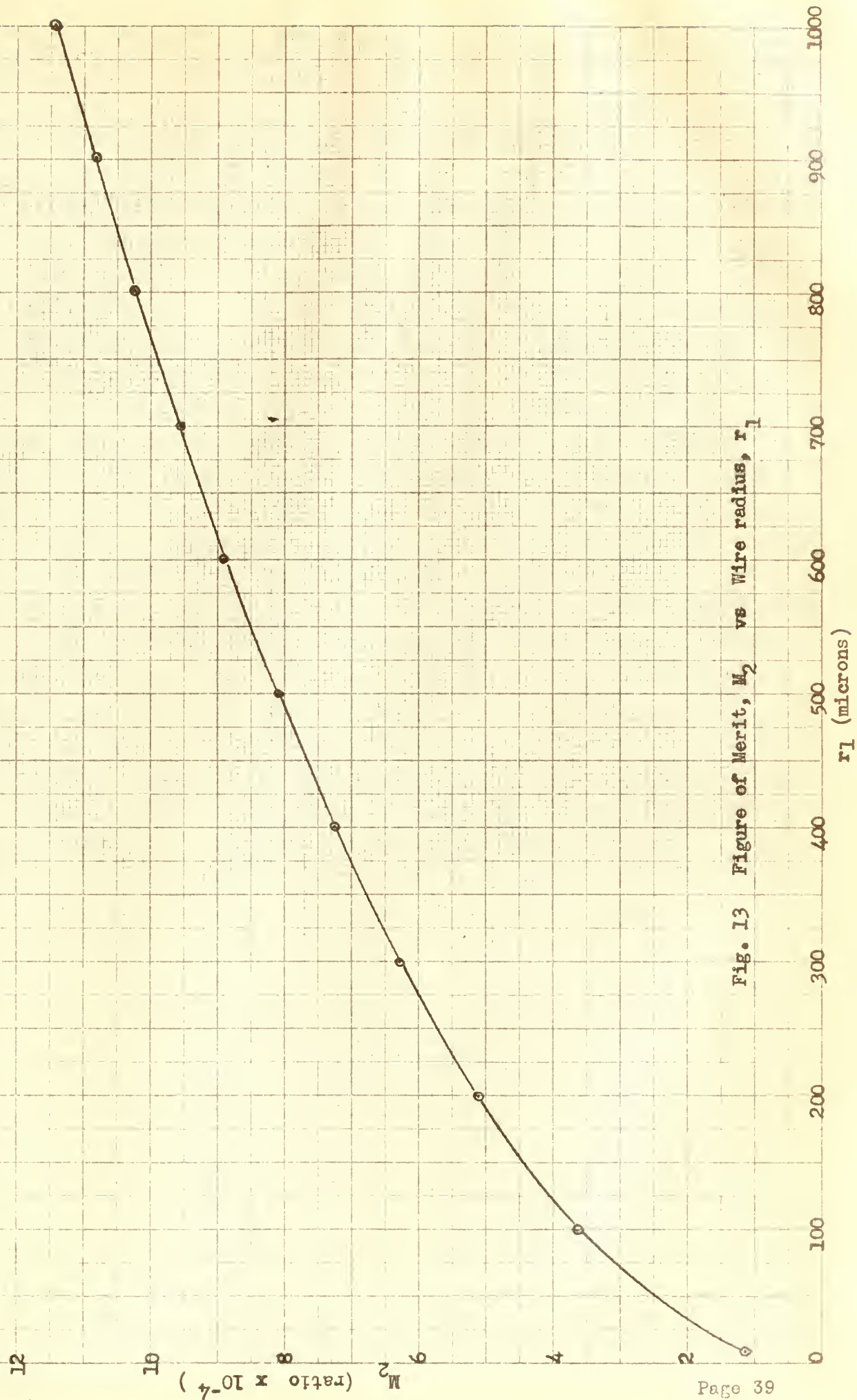


Fig. 13 Figure of Merit, M_2 vs Wire radius, r_1

BIBLIOGRAPHY

1. W. P. Allis, M. A. Herlin, Thermodynamics and Statistical Mechanics, McGraw-Hill, 1952.
2. P. G. Fellgett, On the Ultimate Sensitivity and Practical Performance of Radiation Detectors, J. Opt. Soc. Amer., Vol. 39, No. 11, pp 970-976, 1949.
3. W. W. Harmon, Fundamentals of Electronic Motion, McGraw-Hill, 1953.
4. R. J. Havens, Theoretical Limit for the Sensitivity of Thermal Radiation Detectors, IRIS Proceedings, Vol. 2, No. 1, June 1957.
5. D. F. Hornig and B. J. O'Keefe, The Design of Fast Thermopiles and the Ultimate Sensitivity of Thermal Detectors, Review of Scientific Instruments, Vol. 18, No. 7, July 1947.
6. R. Clark Jones, A New Classification System for Radiation Detectors, J. Opt. Soc. Amer., Vol. 39, No. 5, pp. 327-343, 1949.
7. R. Clark Jones, Factors of Merit for Radiation Detectors, J. Opt. Soc. Amer., Vol. 39, No. 5, pp. 344-356, 1949.
8. R. Clark Jones, Performance of Detectors for Visible and Infrared Radiation, Advances in Electronics, Vol. V, pp 1-96, Academic Press, 1953.
9. H. Margenau, G. M. Murphy, The Mathematics of Physics and Chemistry, F. Van Nostrand Co., 1943.
10. R. B. McQuistan, On an Approximation to Sinusoidal Modulation, J. Opt. Soc. Amer., Vol. 48, No. 1, pp. 63-66, 1958.
11. B. O. Pierce, A Short Table of Integrals, 3rd Ed., Ginn & Co., 1929.
12. R. A. Smith, F. E. Jones, R. P. Chasmar, The Detection and Measurement of Infra-red Radiation, Oxford, 1957.
13. W. R. Smythe, Static and Dynamic Electricity, 2nd Ed., McGraw-Hill, 1950.
14. K. R. Spangenberg, Vacuum Tubes, McGraw-Hill, 1948.
15. J. D. Strong, Procedures in Experimental Physics, London & Glasgow.
16. Aviation Week, Mar., 4, 11, 18, 1957.
17. Handbook of Chemistry and Physics, 37th Ed., 1955-1956, Chemical Rubber Co.
18. Rand Report, R-297, (Confidential)

19. Reference Data for Radio Engineers, 4th Ed., International Telephone and Telegraph Corp., 1956.

APPENDIX I

THE MAGNETIC FLUX DENSITY OF A CURRENT LOOP

The magnetic flux density produced in a single loop by a current I can be determined as shown in Smythe⁽¹³⁾. By symmetry, we know that \bar{A} , magnetic vector potential is independent of ϕ . Therefore P is chosen to be in the xz -plane with $\phi = 0$, for convenience. By paring \bar{ds} at $\pm \phi$ we see that the only component of \bar{A} that exists is \bar{A}_ϕ

$$\begin{aligned} A_\phi &= \frac{\mu I}{4\pi} \oint \frac{ds_\phi}{r} \\ &= \frac{\mu I}{2\pi} \int_0^\pi \frac{a \cos \phi d\phi}{(a^2 + \rho^2 + z^2 - 2a\rho \cos \phi)^{\frac{1}{2}}} \end{aligned}$$

$$\text{Let } \phi = \pi - 2\theta$$

$$d\phi = 2 d\theta$$

$$\text{then } A_\phi = \frac{\mu a I}{\pi} \int_0^{\frac{\pi}{2}} \frac{(2 \sin^2 \theta - 1) d\theta}{[(a + \rho)^2 + z^2 - 4a\rho \sin^2 \theta]^{\frac{1}{2}}}$$

$$\text{let } k^2 = \frac{4a\rho}{(a + \rho)^2 + z^2} \quad \text{to give elliptic form to the integral.}$$

$$2 \sin^2 \theta - 1 = \frac{2}{k^2} \left[k^2 \sin^2 \theta - 1 + 1 - \frac{k^2}{2} \right]$$

$$= \left[\frac{2}{k^2} - 1 \right] - \frac{2}{k^2} \left[(1 - k^2 \sin^2 \theta) \right]$$

Substituting in the integral gives

$$A_\phi = \frac{\mu a I}{\pi k} \frac{1}{2 \sqrt{a\rho}} \left[\left(\frac{2}{k^2} - 1 \right) K - \frac{2}{k^2} E \right]$$

where K , E are complete elliptic integrals of the first and second kinds,

respectively.

Solving for \bar{B} :

$$\bar{B} = \nabla \times \bar{A} \text{ gives}$$

$$B_{\rho} = -\frac{1}{\rho} \frac{\partial}{\partial z} (\rho A_{\phi}) + \frac{1}{\rho} \frac{\partial}{\partial \phi} (A_z) = -\frac{\partial A_{\phi}}{\partial z}$$

$$B_z = -\frac{1}{\rho} \frac{\partial}{\partial \phi} (A_{\rho}) + \frac{1}{\rho} \frac{\partial}{\partial \rho} (\rho A_{\phi}) = \frac{1}{\rho} \frac{\partial}{\partial \rho} (\rho A_{\phi})$$

where

$$\frac{\partial K}{\partial k} = \frac{E}{k(1-k^2)} - \frac{K}{k} ; \quad \frac{\partial E}{\partial k} = \frac{E}{k} - \frac{K}{k}$$

$$\frac{\partial k}{\partial z} = -\frac{zk^2}{4a\rho} ; \quad \frac{\partial k}{\partial \rho} = \frac{k}{a\rho} - \frac{k^3}{4\rho} - \frac{k^3}{4a}$$

Carrying out the indicated operations gives the magnetic flux density in the final form of

$$B_{\rho} = \frac{\mu I}{2\pi} \frac{z}{[(a+\rho)^2 + z^2]^{\frac{1}{2}}} \left[-K + \frac{a^2 - \rho^2 + z^2}{(a-\rho)^2 + z^2} E \right]$$

$$B_z = \frac{\mu I}{2\pi} \frac{1}{[(a+\rho)^2 + z^2]^{\frac{1}{2}}} \left[K + \frac{a^2 - \rho^2 - z^2}{(a-\rho)^2 + z^2} E \right]$$

We are interested only in the B field perpendicular to the electronic motion (B_z). If we express ρ and z as a percent of a and normalize B_z we have a convenient form for plotting. (Fig. 14.)

$$B = B_z \frac{2\pi a}{\mu I} = \frac{1}{[(1+\rho)^2 + z^2]^{\frac{1}{2}}} \left[K + \frac{1-\rho^2-z^2}{(1-\rho)^2 + z^2} E \right]$$

$$B = M (K + NE)$$

$$\text{and } k = \left[\frac{4\rho}{(1+\rho)^2 + z^2} \right]^{\frac{1}{2}}$$

By graphical integration the approximate average B_z has been found for various values of distance z of the electron path from the plane of the loop in terms of the wire radius.

TABLE III

z	B	B_z	n
r_1	2	$\frac{\mu I}{\pi a}$	1
$2r_1$	1.5	$\frac{3}{4} \frac{\mu I}{\pi a}$	$\frac{3}{4}$
$3r_1$	1	$\frac{\mu I}{2 \pi a}$	$\frac{1}{2}$
$4r_1$	0.667	$\frac{\mu I}{3 \pi a}$	$\frac{1}{3}$
$5r_1$	0.5	$\frac{\mu I}{4 \pi a}$	$\frac{1}{4}$

From Table III we can derive a general form

$$B_z \Big|_{\text{ave}} = n \frac{\mu I}{\pi a}$$

where n may be determined for any particular z .

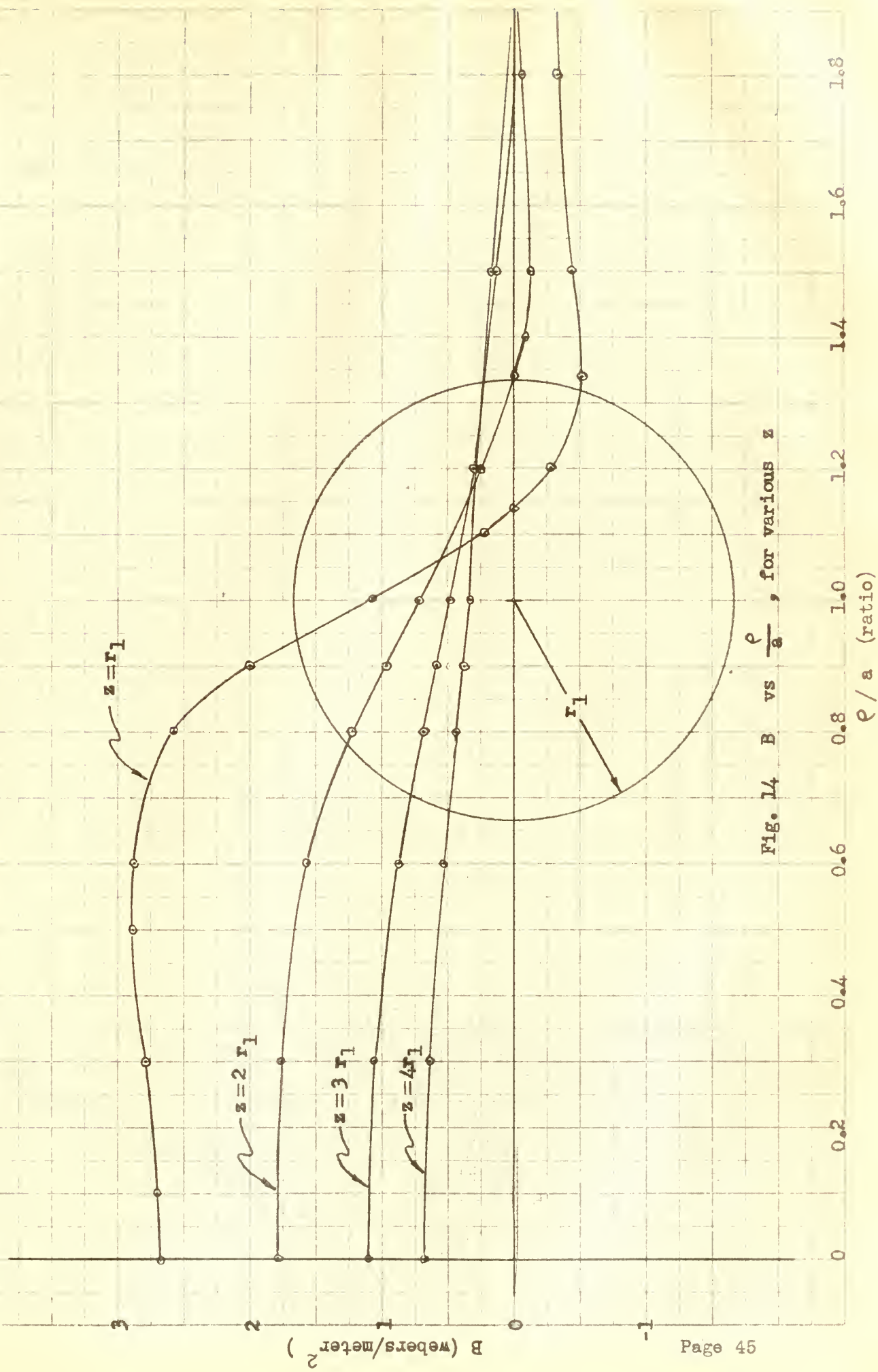


Fig. 14 B vs $\frac{\rho}{a}$, for various z

Fig. 15 (a) z/r vs r_L , for various d_o

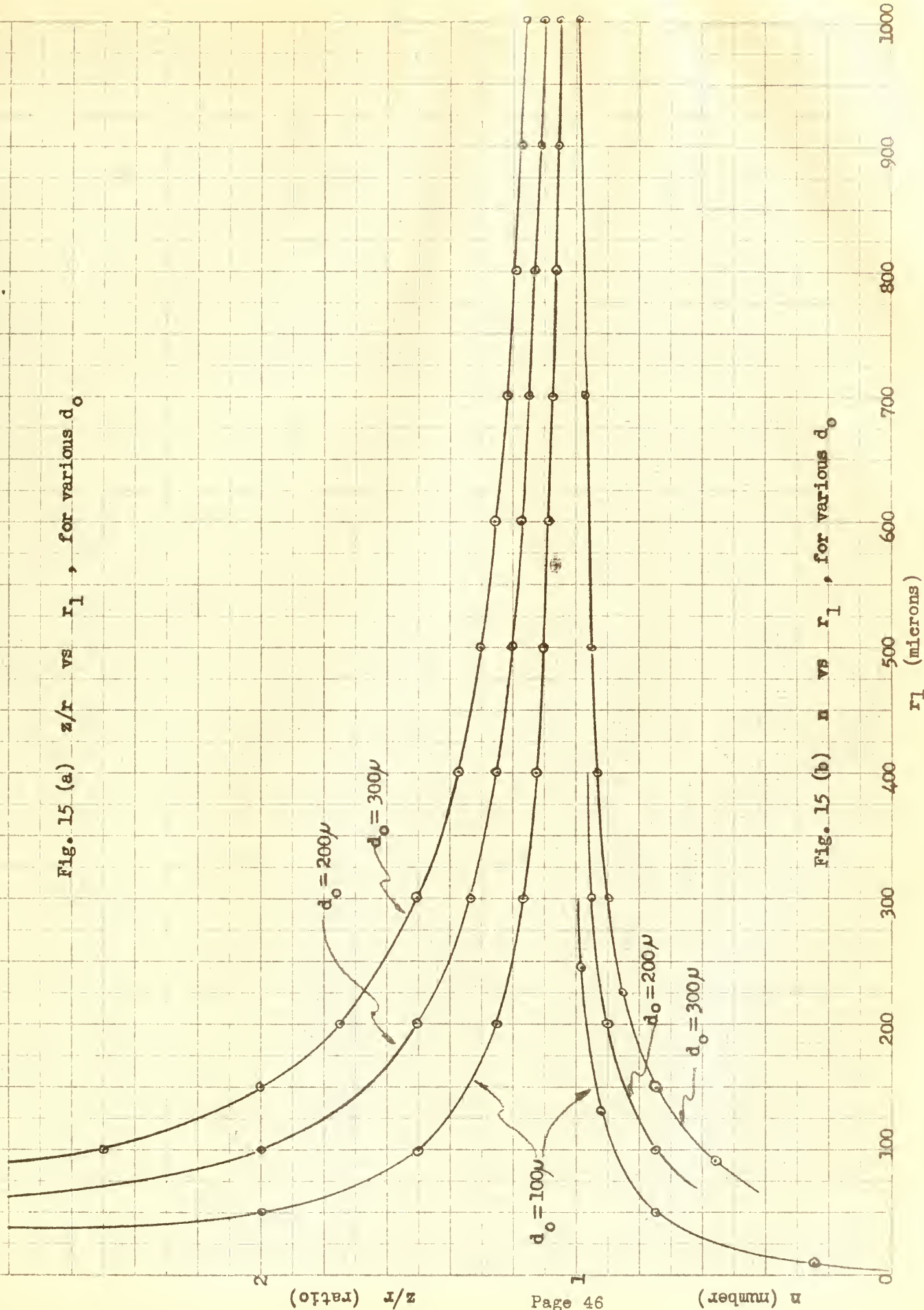
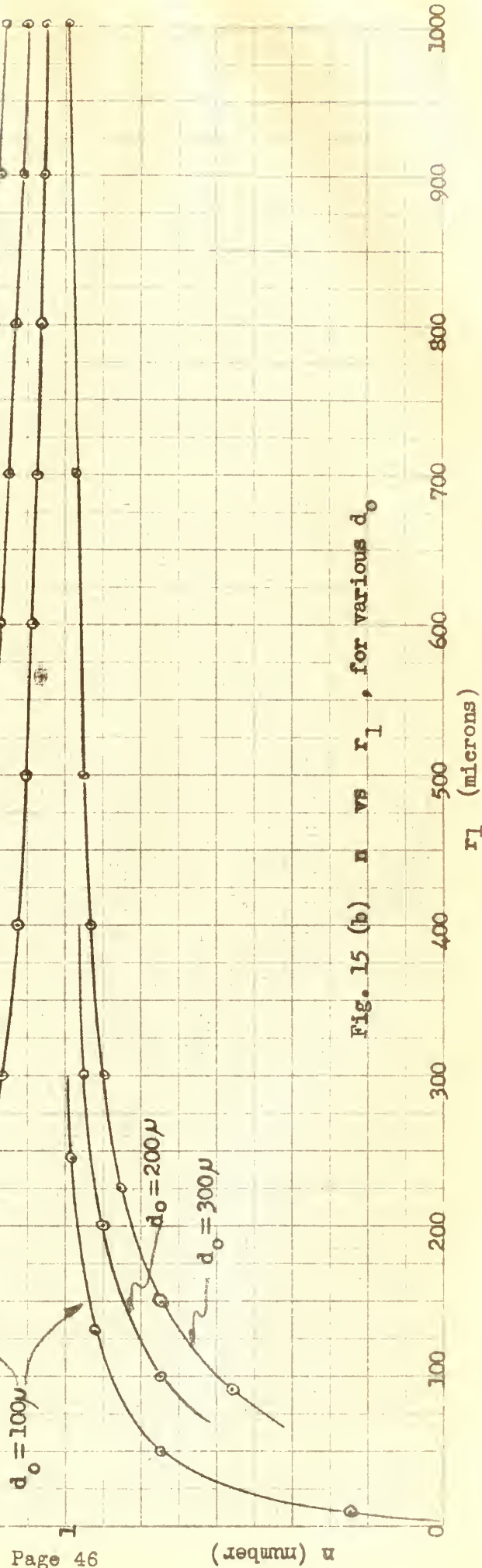


Fig. 15 (b) n vs r_L , for various d_o



APPENDIX II

SOLUTION OF DIFFUSION EQUATION

The diffusion equation represents the temperature change caused by heat flow in a medium, and is given by

$$\frac{\partial \Delta T}{\partial t} = \frac{K}{\rho s} \nabla^2 (\Delta T)$$

For flow constrained within a wire, with no heat transfer at the surface, we have one-dimensional flow along the axis giving

$$\frac{\partial \Delta T}{\partial t} = \frac{K}{\rho s} \frac{\partial^2 \Delta T}{\partial x^2}$$

Solving, let $\Delta T = X(x) Y(t)$

$$\frac{\partial \Delta T}{\partial t} = \dot{X}Y$$

$$\frac{\partial \Delta T}{\partial x} = YX'$$

$$\frac{\partial^2 \Delta T}{\partial x^2} = YX''$$

Substituting $\dot{X}Y = \frac{K}{\rho s} YX''$

$$\frac{\dot{Y}}{Y} = \frac{K}{\rho s} \frac{X''}{X}$$

Let $\frac{\dot{Y}}{Y} = a$; $\frac{X''}{X} = \lambda^2$

then: $Y = Ae^{at}$

$$X = B \sinh(\lambda x + \psi)$$

$$\Delta T(x, t) = XY$$

$$= AB e^{at} \sinh(\lambda x + \psi)$$

For initial conditions, let

$$(1) \Delta T(0, t) = 0$$

$$(2) \Delta T(0, t) = \Delta T(t)$$

From (1) ; $\sinh (\lambda l + \varphi) = 0$

$$\varphi = -\lambda l$$

$$\Delta T(x, t) = AB e^{at} \sinh \lambda (x - l)$$

From (2) $\Delta T(t) = -ABe^{at} \sinh \lambda l$

$$AB = \frac{-\Delta T(t)}{e^{at} \sinh \lambda l}$$

$$\Delta T(x, t) = \Delta T(t) \frac{\sinh \lambda (l-x)}{\sinh \lambda l}$$

$$\Delta W = -AK \left. \frac{\partial \Delta T(x, t)}{\partial x} \right|_{x=0} = Q \Delta T$$

$$\begin{aligned} \Delta W &= \lambda AK \Delta T(t) \frac{\cosh \lambda l}{\sinh \lambda l} \\ &= [\lambda AK \operatorname{ctnh} \lambda l] \Delta T \end{aligned}$$

$$Q = \lambda AK \operatorname{ctnh} \lambda l$$

$$\cong \lambda AK \left[\frac{1}{\lambda l} + \frac{\lambda l}{3} \right]$$

$$= \frac{AK}{l} + \frac{AK l \lambda^2}{3}$$

Two special cases:

Case I Steady state (step function of ΔT after transient has disappeared).

$$\frac{\partial \Delta T}{\partial t} = 0$$

$$\frac{\partial^2 \Delta T}{\partial x^2} = 0$$

$$\Delta T = C_1 x + C_2$$

Condition 1 $\Delta T(l) = 0$; $C_2 = -C_1 l$

Condition 2 $\Delta T = \Delta T_0 = C_1 (0 - l)$

$$\Delta T(x) = \Delta T_0 \left(\frac{l-x}{l} \right)$$

$$\Delta W = -AK \left. \frac{\partial \Delta T}{\partial x} \right|_{x=0} = Q \Delta T$$

$$Q = -AK \left(-\frac{1}{l} \right)$$

$$= G = \frac{AK}{l} \quad \text{conductance}$$

Case II Sinusoidal function ($e^{j\omega t}$)

This gives $a = j\omega$

$$\lambda^2 = \frac{j\omega \rho s}{K}$$

$$Q = G + j\omega C = \frac{AK}{l} + j\omega \frac{A \rho s}{3}$$

$$G = \frac{AK}{l} ; C = \frac{A \rho s}{3}$$

For $\omega = 0$ we again have the steady state solution.

When $a = j\omega$

$$\lambda^2 = \frac{j\omega \rho s}{K}$$

$$\lambda l = \sqrt{\frac{\omega \rho s}{2K}} (1 + j) l$$

Let $L = \sqrt{\frac{2K}{\omega \rho s}} = \sqrt{\frac{K}{\pi \rho s f}}$ has dimension of length ,

$$\lambda l = \frac{l}{L} (1 + j)$$

A plot of L vs. f for Bi and Bi \neq Sn shows that Bi \neq Sn limits the length and the frequency of chopping. (Fig. 16).

If $l \gg L$; $\cosh \lambda l \approx 1$

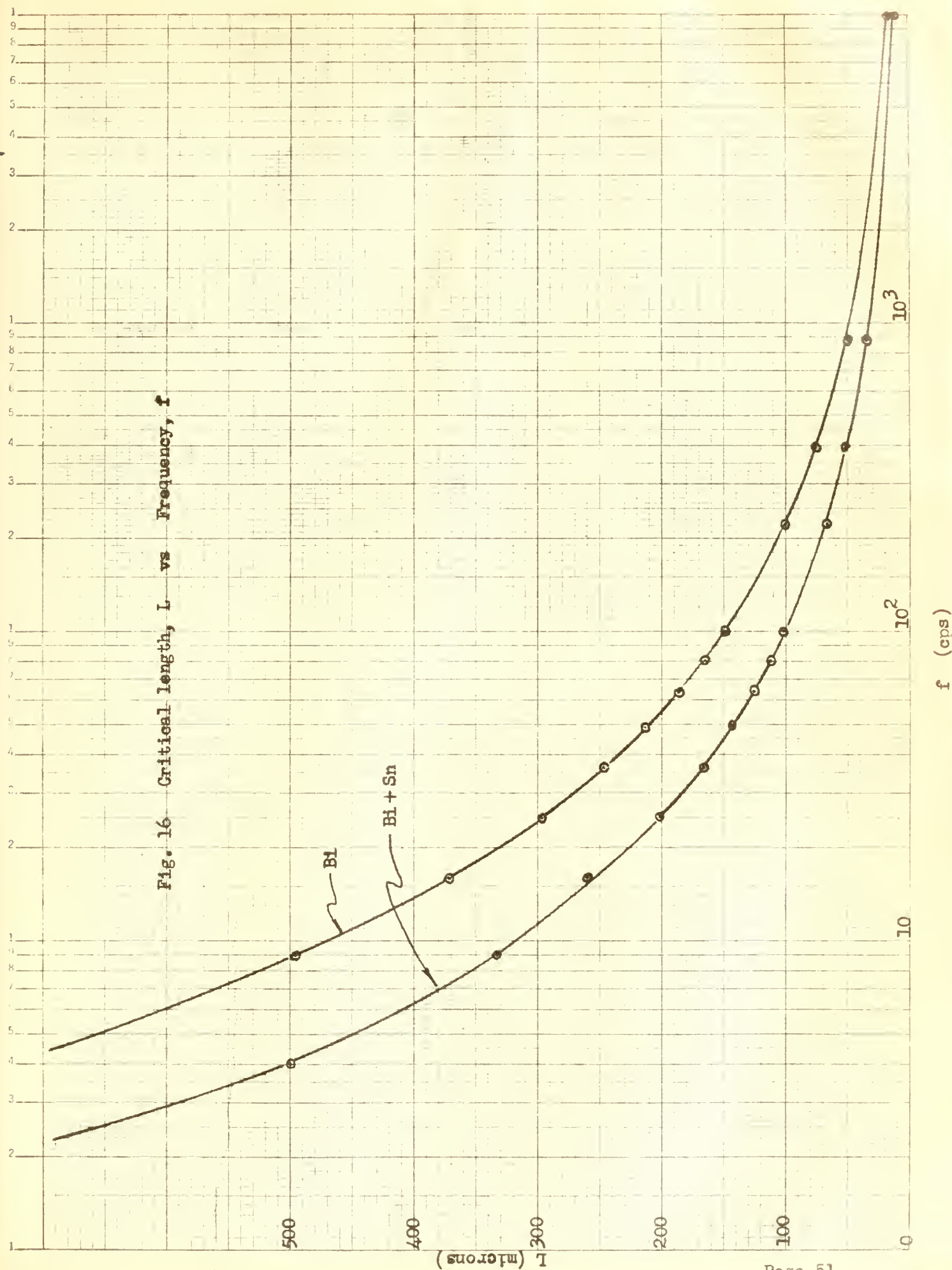
$$Q = AK \lambda = \frac{AK}{L} (1 + j)$$

$$G = \omega C = \frac{AK}{L}$$

$$\text{If } l \ll L; \operatorname{ctnh} \lambda l \approx \frac{1}{\lambda l} \neq \frac{\lambda l}{3}$$

$$Q = \frac{AK}{l} \neq j \frac{\omega A l \epsilon s}{3}$$

Fig. 16 Critical length, L vs Frequency, f



APPENDIX III

ATMOSPHERIC TRANSMISSION OF INFRARED

The spectral distribution of IR energy is a function of temperature and wavelength as given by

$$F(t, \lambda) = \frac{2\pi hc^2}{e^{\frac{ch}{\lambda kT}} - 1} \cdot \frac{d\lambda}{\lambda^5} \text{ watts/meter}^2$$

$$\cong 2\pi hc^2 e^{-\frac{ch}{\lambda kT}} \frac{d\lambda}{\lambda^5}$$

By integrating this function over the discrete wavelengths of Fig. 17, a body of unit area at the temperature $T = 300^\circ \text{K}$ has the following energies:

	No absorption	Atmospheric absorption
$W_1 (0 - 1.3) = 3.6 \times 10^{-10}$		1.8×10^{-10}
$W_2 (1.5 - 1.8) = 3.71 \times 10^{-6}$		2.66×10^{-6}
$W_3 (2.1 - 2.5) = 1.41 \times 10^{-3}$		1.13×10^{-3}
$W_4 (3.3 - 4.2) = 1.37$		1.243
$W_5 (4.5 - 4.9) = 1.67$		1.17
$W_6 (8 - 13) = 133$		92.8

The energy in the FIR region is 29% of the total energy radiated (= 459 watts). Atmospheric absorption reduces this to 20% of the total power which is detectable. The energy within the other bands (NIR and MIR) is only one-half of one percent of the total radiated energy.

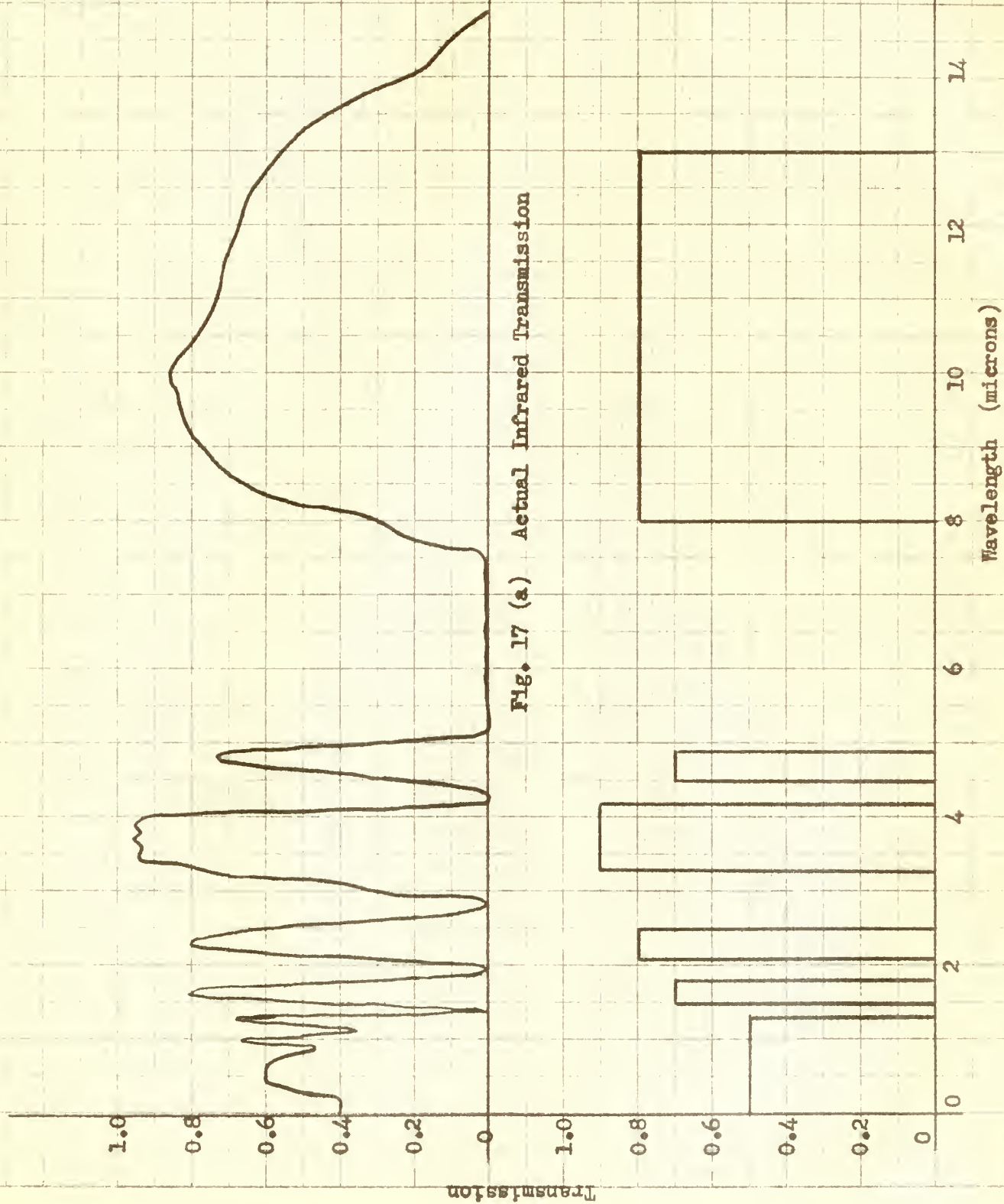
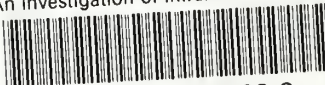


Fig. 17 (a) Actual Infrared Transmission

Fig. 17 (b) Approximate Infrared Transmission

thesB588

An investigation of infrared detection b



3 2768 002 07683 8
DUDLEY KNOX LIBRARY